



Published in final edited form as:

*Cancer Immunol Res.* 2019 March ; 7(3): 363–375. doi:10.1158/2326-6066.CIR-18-0572.

## NK cells expressing a chimeric activating receptor eliminate MDSCs and rescue impaired CAR-T cell activity against solid tumors

Robin Parihar<sup>1,2,\*</sup>, Charlotte Rivas<sup>1,2</sup>, Mai Huynh<sup>1</sup>, Bilal Omer<sup>1,2</sup>, Natalya Lapteva<sup>1</sup>, Leonid S. Metelitsa<sup>1,2,3</sup>, Stephen M. Gottschalk<sup>4</sup>, Cliona M. Rooney<sup>1,2,3,5</sup>

<sup>1</sup>Center for Cell and Gene Therapy, Texas Children's Hospital, Houston Methodist Hospital, and Baylor College of Medicine, Houston, TX, USA

<sup>2</sup>Department of Pediatrics, Section of Hematology-Oncology, Baylor College of Medicine, TN, USA

<sup>3</sup>Department of Pathology, Division of Immunology, Baylor College of Medicine, TN, USA

<sup>4</sup>St. Jude Children's Research Hospital, Memphis, TN, USA

<sup>5</sup>Department of Molecular Virology and Immunology, Baylor College of Medicine, Houston, TX, USA.

### Abstract

Solid tumors are refractory to cellular immunotherapies in part because they contain suppressive immune effectors such as myeloid-derived suppressor cells (MDSCs) that inhibit cytotoxic lymphocytes. Strategies to reverse the suppressive tumor microenvironment (TME) should also attract and activate immune effectors with antitumor activity. To address this need, we developed gene-modified natural killer (NK) cells bearing a chimeric receptor in which the activating receptor NKG2D is fused to the cytotoxic  $\zeta$ -chain of the T-cell receptor (NKG2D. $\zeta$ ). NKG2D. $\zeta$ -NK cells target MDSCs, which overexpress NKG2D ligands within the TME. We examined the ability of NKG2D. $\zeta$ -NK cells to eliminate MDSCs in a xenograft TME model and improve the antitumor function of tumor-directed chimeric antigen receptor (CAR)-modified T cells. We show that NKG2D. $\zeta$ -NK cells are cytotoxic against MDSCs, but spare NKG2D ligand-expressing normal tissues. NKG2D. $\zeta$ -NK cells, but not unmodified NK cells, secrete pro-inflammatory cytokines and chemokines in response to MDSCs at the tumor site and improve infiltration and antitumor activity of subsequently infused CAR-T cells, even in tumors for which an immunosuppressive TME is an impediment to treatment. Unlike endogenous NKG2D, NKG2D. $\zeta$  is not susceptible to TME-mediated down-modulation and thus maintains its function even within suppressive microenvironments. As clinical confirmation, NKG2D. $\zeta$ -NK cells generated from

\*Address correspondence to: Robin Parihar, MD, PhD, Center for Cell and Gene Therapy, Baylor College of Medicine, 1102 Bates St, Suite 1770.02, Houston, TX 77030, Tel: +1- 832-824-4746 Fax: +1-832-825-4732, rxpariha@txch.org.

#### AUTHOR CONTRIBUTIONS

R.P., C.R., N.L., and C.M.R. designed experiments; R.P. and C.R. performed experiments; S.G., M.H. and B.O. provided retroviral constructs and technical expertise; L.M., S.G., and C.M.R. provided expert scientific guidance; R.P. and C.M.R. wrote the manuscript; All authors approved the final manuscript.

The authors declare no potential conflicts of interest.

patients with neuroblastoma killed autologous intra-tumoral MDSCs capable of suppressing CAR-T function. A combination therapy for solid tumors that includes both NKG2D.ζ–NK cells and CAR-T cells may improve responses over therapies based on CAR-T cells alone.

### Keywords

NK cells; MDSCs; CAR T cells; NKG2D; Solid Tumors; Neuroblastoma

## INTRODUCTION

T lymphocytes can be engineered to target tumor-associated antigens by forced expression of CARs (1). Although successful when directed against leukemia-associated antigens such as CD19 (2, 3), CAR-T cell therapy for solid tumors has been less effective, with best responses in patients with minimal disease (4, 5). Solid tumors recruit inhibitory cells such as myeloid-derived suppressor cells (MDSCs) (6). These immature myeloid cells are a component of innate immunity and strengthen the suppressive TME (7, 8). The frequency of circulating or intra-tumoral MDSCs correlates with cancer stage, disease progression, and resistance to standard chemo- and radio-therapies (9). Hence, MDSCs are worth targeting in the quest to enhance CAR-T cell efficacy against solid tumors.

Natural killer (NK) cells, a lymphoid component of the innate immune system, produce MHC-unrestricted cytotoxicity and secrete pro-inflammatory cytokines and chemokines (10). NK cells also modulate the activity of antigen-presenting myeloid cells within lymphoid organs, and recruit and activate effector T cells at sites of inflammation (11, 12). NK cells express NKG2D, a cytotoxicity receptor that is activated by non-classical MHC molecules expressed on cells stressed by events such as DNA damage, hypoxia, or viral infection (13). NKG2D ligands are overexpressed on several solid tumors and on tumor-infiltrating MDSCs (14). NK cells, therefore, could alter the TME in favor of an antitumor response by eliminating suppressive elements such as MDSCs. However, the NKG2D cytotoxic adapter molecule, DAP10, is downregulated by suppressive molecules of the TME, such as TGFβ (15), limiting the antitumor functions of NK cells.

To overcome the repressive effect of the solid TME on NKG2D function, we used a retroviral vector to modify NK cells with a chimeric NKG2D receptor (NKG2D.ζ) comprising the extracellular domain of the native NKG2D molecule fused to the intracellular cytotoxic ζ-chain of the T-cell receptor (16). We hypothesized that primary human NK cells expressing NKG2D.ζ (NKG2D.ζ–NK cells) would maintain NKG2D.ζ expression within the suppressive TME, kill NKG2D ligand-expressing MDSCs, secrete pro-inflammatory cytokines and chemokines, and recruit and activate effector cells, including CAR-T cells, derived from the adaptive immune system. These benefits are not attainable from NK cells expressing the native NKG2D receptor as its functions are downmodulated in the TME. Here we show that when NK cells express NKG2D.ζ, immune suppression is sufficiently countered to enable tumor-specific CAR-T cells to persist within the TME and eradicate otherwise resistant tumors.

## MATERIALS AND METHODS

### Cytokines, cell lines, and antibodies.

Recombinant human interleukin (IL)2 was obtained from National Cancer Institute Biologic Resources Branch (Frederick, MD). Recombinant human IL6, GM-CSF, IL7, and IL15 were purchased from Peprotech (Rocky Hill, NJ, USA). The human neuroblastoma cell line LAN-1 was purchased from American Type Culture Collection (Manassas, VA, USA) and cultured in DMEM culture medium supplemented with 2 mM L-glutamine (Gibco-BRL) and 10% FBS (Hyclone, Waltham, MA, USA). The human CML cell line K562 was purchased from American Type Culture Collection and cultured in complete-RPMI culture medium composed of RPMI-1640 medium (Hyclone) supplemented with 2 mM L-glutamine and 10% FBS. A modified version of parental K562 cells, genetically modified to express a membrane-bound version of IL15 and 41BB-ligand, K562-mb15–41BB-L, was kindly provided by Dr. Dario Campana (National University of Singapore). All cell lines were verified by either genetic or flow cytometry-based methods (LAN-1 and K562 authenticated by ATCC in 2009) and tested for mycoplasma contamination monthly via MycoAlert (Lonza) mycoplasma enzyme detection kit (last mycoplasma testing of LAN-1, K562 parental line, and K562-mb15–41BB-L on November 2, 2018; all negative). All cell lines were used within one month of thawing from early-passage (< 3 passages of original vial) lots.

### CAR-encoding retroviral vectors.

The construction of the SFG-retroviral vector encoding GD2-CAR.41BB.ζ, as shown in Supplementary Fig. S1A, was previously described (17). The SFG-retroviral vector encoding NKG2D.ζ, an internal ribosomal entry site (IRES), and truncated CD19 (tCD19), was generated by sub-cloning NKG2D.ζ from a retroviral vector (18) kindly provided by Dr. Charles L. Sentman (Dartmouth Geisel School of Medicine, Hanover, NH, USA) into pSFG.IRES.tCD19 (19). RD114-speudotyped viral particles were produced by transient transfection in 293T cells, as previously described (20).

### Expansion and retroviral transduction of human NK and T cells.

Human NK cells were activated, transduced with retroviral constructs (Fig. 1A) and expanded as previously described by our laboratory (21). Briefly, peripheral blood mononuclear cells (PBMCs) obtained from healthy donors under Baylor College of Medicine IRB-approved protocols, were cocultured with irradiated (100 Gy) K562-mb15–41BB-L at a 1:10 (NK cell:irradiated tumor cell) ratio in G-Rex<sup>®</sup> cell culture devices (Wilson Wolf, St. Paul, MN, USA) for 4 days in Stem Cell Growth Medium (CellGenix) supplemented with 10% FBS and 500 IU/mL IL2. Cell suspensions on day 4 (containing 50–70% expanded/activated NK cells) were transduced with SFG-based retroviral vectors, as previously described (22). The transduced cell population was then subjected to secondary expansion to generate adequate cell numbers for experiments in G-Rex<sup>®</sup> devices at the same NK cell:irradiated tumor cell ratio with 100 IU/mL IL2. This 17-day human gene-modified NK cell protocol resulted in > 97% pure CD56<sup>+</sup>/CD3<sup>-</sup> NK cell population with avg. 77.4% ± 18.2% (n = 25) of NK cells transduced with the construct of interest. For

most experiments, transduced NK cells were purified to > 95% by magnetic column selection of truncated CD19 selection marker-positive cells.

For production of GD2.CAR-T cells (autologous to MDSCs and NK cells), PBMCs from healthy donors were suspended in T-cell medium (TCM) consisting of RPMI-1640 supplemented with 45% Click's Medium (Gibco-BRL), 10% FBS, and 2 mM L-glutamine, and cultured in wells pre-coated with CD3 (OKT3, CRL-8001, American Type Culture Collection) and CD28 (Clone CD28.2, BD Biosciences) antibodies for activation. Human IL15 and IL7 were added on day +1, and cells underwent retroviral transduction on day +2, as previously described (22). T-cells were used for experiments between days +9 to +14 post-transduction, with phenotype as shown in Supplementary Figs. S1B–C.

### Induction and enrichment of human MDSCs.

Our method for *ex vivo* generation of human PBMC-derived MDSCs was derived from published reports (23), with slight modifications. Briefly, PBMCs were sequentially depleted of CD25<sup>hi</sup>-expressing cells and CD3-expressing cells by magnetic column separation (Miltenyi Biotec). Resultant CD25<sup>lo/-</sup>, CD3<sup>-</sup> PBMCs were plated at  $4 \times 10^6$  cells/mL in complete-RPMI medium with human IL6 and GM-CSF (both at 20 ng/mL) onto 12-well culture plates (Sigma Corning) at 1 mL/well. Plates were incubated for 7 days with medium and cytokines being replenished on days 3 and 5. Resultant cells were harvested by gentle scraping and MDSCs were purified by magnetic selection using CD33 magnetic microbeads (Miltenyi Biotec). Cells were analyzed by multi-color flow cytometry for CD33, CD14, CD15, HLA-DR, CD11b, CD83, and CD163 (BD Biosciences). MDSCs were defined as either monocytic (M-MDSCs; CD14<sup>+</sup>, HLA-DR<sup>low/-</sup>), PMN-MDSCs (CD14<sup>-</sup>, CD15<sup>+</sup>, CD11b<sup>+</sup>), or early-stage MDSCs (lineage<sup>-</sup>, HLA-DR<sup>low/-</sup>, CD33<sup>+</sup>), as per published guidelines (24). In addition to the above markers, MDSCs were stained for PD-L1, PD-L2, and NKG2D ligands via an NKG2D-Fc chimera (BD Biosciences) followed by FITC-labeled anti-Fc. This pan-ligand staining approach was determined to be the most efficient way to assess NKG2D ligand expression on human MDSCs because (1.) NKG2D ligand expression had not previously been reported for human MDSCs and thus simultaneous evaluation of the eight different NKG2D ligands would have been required, and (2.) we found poor reproducibility in staining patterns using individual commercially-available ligand antibodies, even within the same donor.

### *In vitro* T-cell suppression assay.

T-cell proliferation was assessed using Cell Trace Violet (Thermo Fisher) dye dilution analysis, as per manufacturer's recommendations. Briefly,  $1 \times 10^5$  Cell Trace Violet-labeled T cells (isolated at the time of MDSC generation) were plated onto 96-well plates in the presence of plate-bound 1  $\mu$ g/mL CD3 and 1  $\mu$ g/mL CD28 antibodies with 50 IU/mL IL2 in the absence or presence of autologous MDSCs or peripheral blood monocytes (as a myeloid cell control) at 1:1, 4:1 and 8:1 T cell:MDSC ratios. In some experiments, only the 4:1 ratio is shown as this was determined as optimal for assessment of suppression. After 4 days of coculture, T cells were labeled with CD3 antibody and assessed for cell division using Cell Trace Violet dye dilution by flow cytometry. Percent suppression was calculated as follows: [(% proliferating T cells in the absence of MDSCs - % proliferating T cells in presence of

MDSCs)/% proliferating T cells in the absence of MDSCs] x 100. Proliferation was defined as % T cells undergoing active division as represented by Cell Trace Violet dilution peaks, as previously described (25).

#### ***In vitro* CAR-T chemotaxis assay.**

Transwell 5- $\mu$ m pore inserts (Corning, Somerset, NJ) for migration experiments were prepared by coating with 0.01% gelatin at 37 °C overnight, followed by 3  $\mu$ g of human fibronectin (Life Technologies, Grand Island, NY) at 37 °C for 3 hours to mimic endothelial and extracellular matrix components, as previously described (26). Briefly,  $2 \times 10^5$  purified GD2.CAR-T cells were placed in 100  $\mu$ L of TCM in the upper chambers of the pre-coated Transwell inserts that were then transferred into wells of a 24-well plate. Culture supernatants (400  $\mu$ L) from NKG2D. $\zeta$  or unmodified NK cells cultured with autologous MDSCs or monocytes, were placed in the lower chambers of the wells. Plain medium or medium supplemented with 1  $\mu$ g/mL of the T-cell recruiting chemokine, MIG, served as negative and positive controls, respectively. The plates were then incubated for 4 hours at 37 °C with 5% CO<sub>2</sub>, followed by a 10-minute incubation at 4 °C to loosen any cells adhering to the undersides of the insert membranes. The fluid in the lower chambers was collected separately and migrated cells were counted using trypan blue exclusion. The cells were analyzed for CAR expression by flow cytometry to confirm phenotype of migrated T cells.

#### ***In vivo* tumor microenvironment model.**

12–16 week old female NSG mice were implanted subcutaneously in the dorsal right flank with  $1 \times 10^6$  Firefly luciferase (Fluc)-expressing LAN-1 neuroblastoma cells admixed with  $3 \times 10^5$  *ex vivo*-generated MDSCs, suspended in 100  $\mu$ L of basement membrane Matrigel (Corning). Matrigel basement membrane was important in keeping tumor and MDSCs confined so as to establish a localized solid TME. 10–14 days later, when tumors measured at least 100 mm<sup>3</sup> by caliper measurement, mice were injected intravenously with  $5 \times 10^6$  GD2.CAR-T cells. Tumor growth was measured twice weekly by live bioluminescence imaging using the IVIS<sup>®</sup> system (IVIS, Xenogen Corporation) 10 minutes after 150 mg/kg D-luciferin (Xenogen)/mouse was injected intraperitoneally. In experiments examining the ability of NKG2D. $\zeta$ -NK cells to reduce intra-tumoral MDSCs,  $1 \times 10^7$  unmodified or NKG2D. $\zeta$ -NK cells were injected intravenously when tumors measured at least 100 mm<sup>3</sup>. At end of experiment, tumors were harvested *en bloc*, digested *ex vivo*, and intra-tumoral human MDSCs (CD33<sup>+</sup>, HLA-DR<sup>low</sup> cells) were enumerated by flow cytometry. The absolute number of human MDSCs within a tumor digest was enumerated per mouse (n = 5 mice/group), compared to pre-treatment MDSC numbers, and presented as mean % MDSCs remaining per treatment group. In experiments examining the effects of NKG2D. $\zeta$ -NK cells on GD2.CAR-T cell antitumor activity,  $5 \times 10^6$  (cell dose chosen to mitigate direct antitumor effects of NK cells) unmodified or NKG2D. $\zeta$ -NK cells were injected intravenously 3 days prior to GD2.CAR-T injection. In GD2.CAR-T cell homing experiments, CAR-T were transduced with GFP-luciferase retroviral construct prior to injection into mice bearing unmodified tumor cells (27). Mice received 5000 IU human IL2 intraperitoneally three times per week for 3 weeks following NK cell injection to promote NK cell survival in NSG mice (28). Tumor size was measured twice weekly with calipers and the mice were imaged for bioluminescence signal from T cells at the same time. Mice were euthanized for excessive

tumor burden, as per protocol guidelines. The animal studies protocol was approved by Baylor College of Medicine Institutional Animal Care and Use Committee and mice were treated in strict accordance with the institutional guidelines for animal care.

### **Immunohistochemistry of neuroblastoma xenografts.**

On day 32 of *in vivo* experiments, animals were sacrificed, tumors were harvested and sectioned bluntly *ex vivo* to separate tumor periphery (outer 1/3 of tumor volume) vs. core (non-necrotic inner 2/3 of tumor volume), and  $n = 5$  sections/tumor sample were analyzed for presence of GD2.CAR-T and NKG2D.ζ-NK cells by H&E and human CD3 and CD57 immunostaining performed by the Human Tissue Acquisition and Pathology Core of Baylor College of Medicine. Lack of CD57 expression on infused GD2.CAR-T was confirmed by flow cytometry prior to administration. CD57 was chosen as the marker for NK cells in tumor tissue in our study because LAN-1 tumors naturally express the prototypical NK marker CD56, truncated CD19 expression was inadequate for *in situ* staining, and CD57 had previously been used as a marker for tissue-localized activated NK cells (29). The number of human CD3+ and CD57+ cells in representative sections of tumors from periphery vs. core of the treatment groups indicated were enumerated per high-powered field (HPF) at 40x magnification and percent of the total number of cells enumerated within tumors found in the periphery vs. core in each treatment group indicated from tumors with and without MDSCs is shown as mean  $\pm$  SEM of  $n = 5$  sections/periphery or core,  $n = 5$  tumors/group.

### **Analysis of intra-tumoral MDSCs from patients with neuroblastoma.**

Tumor tissue and matched peripheral blood of neuroblastoma patients obtained in the context of a specimen/laboratory study after patient identification had been removed were thawed and analyzed for MDSC subsets by flow cytometry or utilized in *in vitro* assays, as described in legends or Results. The tissue acquisition protocol was performed after review and approval by the Baylor College of Medicine Institutional Review Board. Briefly, subjects with a diagnosis of high-risk or intermediate-risk neuroblastoma were eligible to participate. Written informed consent, or appropriate assent for participation, in accordance with the Declaration of Helsinki was obtained from each subject or subject's guardian for procurement of patient blood and tumor tissue and for subsequent analyses of stored patient materials.

### **Statistics.**

Data are presented as mean  $\pm$  SEM of either experimental replicates or number of donors, as indicated. Paired two-tailed t-test was used to determine significance of differences between means with  $p < 0.05$  indicating a significant difference. For *in vivo* bioluminescence, changes in tumor radiance from baseline at each time point were calculated and compared between groups using two-sample t-test. Multiple group comparisons were conducted via ANOVA via GraphPad Prism v7 software. Survival determined from the time of tumor cell injection was analyzed by Kaplan-Meier and differences in survival between groups were compared by the log-rank test.

## RESULTS

### **NKG2D.ζ NK cells expand and have cytotoxicity against target cells.**

To increase killing of NKG2D ligand-expressing MDSCs, we generated primary human NK cells stably expressing NKG2D.ζ and a truncated CD19 (tCD19) marker from a retroviral vector (Fig. 1A). NK cells were expanded from PBMCs obtained from normal donors, transduced with retroviral construct expressing chimeric NKG2D, then cultured for 3 additional days. Transduction efficiency, as measured by the expression of tCD19 on CD56<sup>+</sup>CD3<sup>-</sup> NK cells after the additional 3 days, was 71.3 ± 16% (n = 25 normal donors) and produced a 5.4 ± 1.1-fold increase in NKG2D expression on the NK cell surface (Fig. 1B–D). NKG2D.ζ–NK cells showed greater cytotoxicity (79.2 ± 5.6%, n = 10 normal donors) against wild-type K562, a highly NK cell-sensitive tumor cell line that naturally expresses NKG2D ligands, than mock vector-transduced (hereafter referred to as, unmodified) NK cells (40.5 ± 2.1%) at 2:1 E:T ratio in a 4-hr cytotoxicity assay (Fig. 1E). In contrast, transgenic NKG2D.ζ expression did not increase NK cell killing of LAN-1 neuroblastoma cells that are marginally NK-sensitive, but lack NKG2D ligands. To determine if *in vitro* expansion affected the cytotoxic function of NKG2D.ζ–NK cells, we secondarily expanded NKG2D.ζ–NK cells for an additional 10-days (Fig. 1F schema). As seen in Fig. 1F, NKG2D.ζ–NK cells expanded (120 ± 7.3-fold by day 17 of culture; n = 10 donors) similarly to unmodified and non-transduced NK cells and maintained stable cytotoxic function between days 7 and 17 of expansion. Thus, we generated and expanded high numbers of primary human NKG2D.ζ-expressing NK cells capable of cytotoxicity against ligand-expressing targets, even after prolonged culture.

### **Transgenic NKG2D.ζ is unaffected by TGFβ or soluble NKG2D ligands.**

Expression of the native NKG2D receptor on NK cells is down-modulated by tumor-derived TGFβ and soluble NKG2D ligands, both of which are abundant in the TME (15, 30) and likely impair NK cell function in solid tumors. To determine the effect of TGFβ and soluble NKG2D ligands on NKG2D.ζ receptor expression and function, we cultured NKG2D.ζ–NK cells in the presence of TGFβ or the soluble NKG2D ligands, MICA and MICB, and examined NKG2D expression and NK cytotoxicity after 24-, 48-, and 72-hours. After exposure to TGFβ or soluble MICA/B, unmodified NK cells significantly down-regulated NKG2D (MFI of 25 vs. 95 in non-exposed NK cells at 48 hours) and were less cytotoxic (20 ± 5.1% killing vs. 40 ± 3.7% killing by non-exposed NK cells at 48 hours) to NKG2D ligand-expressing K562 targets (Fig. 2A, B). In contrast, NKG2D.ζ–NK cells maintained NKG2D expression and cytotoxicity after exposure to the same concentrations of TGFβ and soluble MICA/B (Fig. 2C, D). This lack of sensitivity to down-regulation by these tumor-associated components should benefit the function of NKG2D.ζ–NK cells within the TME.

### **Human MDSCs express NKG2D ligands and are killed by NKG2D.ζ–NK cells.**

To study the effects of human NK cells on autologous MDSCs, we generated human MDSCs by culture of CD3<sup>-</sup>/CD25<sup>lo</sup> PBMC with IL6 plus GM-CSF for 7 days, followed by CD33<sup>+</sup> selection, as described in the Methods. The phenotypic characterization of these MDSCs and confirmation of their suppressive capacity is shown in Supplementary Fig. S2. Routinely, our *ex vivo*-generated MDSCs contained monocytic (M)-MDSC and early(e)-

MDSC subsets, with few (avg. < 1%) polymorphonuclear (PMN)-MDSCs (Supplementary Fig. S2A), roughly reflecting the subset composition reported in patients with solid tumors (9, 31). The MDSCs expressed the suppressive factors TGF $\beta$ , IL6, IL10, and PDL-1 in amounts often greater than tumor cells (Supplementary Figs. S2B–C), and suppressed proliferation and cytokine secretion by autologous T cells stimulated with plate-bound CD3/CD28 antibodies (Supplementary Figs. S2D–E) and by 2<sup>nd</sup> generation GD2.CAR-T cells encoding 4–1BB and CD3- $\zeta$  endodomains stimulated with the GD2<sup>+</sup> tumor line LAN-1 (Supplementary Figs. S2F–G). As seen in Fig. 3A, MDSCs expressed as much or more NKG2D ligand than the positive control tumor line, K562 (ligand MFI of 78.2 vs. 29.7, respectively). Freshly isolated peripheral blood T cells did not express NKG2D ligands, whereas immature and mature dendritic cells expressed little, consistent with previous data (13). The neuroblastoma cell line, LAN-1, subsequently used in our *in vivo* TME model, did not express NKG2D ligands.

To evaluate MDSC susceptibility to killing by NKG2D. $\zeta$ -NK cells, we performed both short- and long-term killing assays. Fig. 3B shows enhanced killing of MDSCs by autologous NKG2D. $\zeta$ -NK cells compared to unmodified NK cells ( $35 \pm 5.5\%$  vs.  $8 \pm 2.4\%$  cytotoxicity, respectively, at an E:T ratio of 5:1) in a 4-hr chromium-release assay. MDSC killing was dependent on NKG2D, as pre-incubation with an NKG2D blocking Ab reduced the cytotoxicity to levels achieved by unmodified NK cells. NKG2D. $\zeta$ -NK cells mediated no cytotoxicity against other autologous immune cells such as freshly-isolated monocytes, monocyte-derived mature dendritic cells, T cells, or B cells (Fig. 3C). Only immature dendritic cells, which expressed little NKG2D ligand (approx. 7% of cells; MFI 11.4), were mildly susceptible to lysis by NKG2D. $\zeta$ -NK cells ( $4.2 \pm 1.7\%$  lysis at an E:T ratio of 20:1). As confirmation of the clinical applicability of our approach, we assessed whether NKG2D. $\zeta$ -NK cells generated from patient PBMCs were able to kill highly suppressive MDSCs isolated from the patient's tumor. Tumor samples obtained from two patients with high-risk neuroblastoma at time of first biopsy/resection contained M-MDSCs (Fig. 3D). NKG2D. $\zeta$ -NK cells generated from patient PBMCs (harvested and frozen at time of tumor sampling) mediated significant cytotoxicity *in vitro* against M-MDSCs purified from patient tumors, whereas unmodified patient NK cells did not (Fig. 3E). These results provide further clinical evidence for the capacity of NKG2D. $\zeta$ -NK cells to eliminate MDSCs in patients with suppressive TMEs.

To determine whether NKG2D. $\zeta$ -NK cells could control MDSC survival in long-term cultures, we cocultured NKG2D. $\zeta$ -NK cells with autologous MDSCs at a 1:1 ratio for 7 days in the presence of low-dose IL2 to maintain NK survival, and quantified each cell type by flow cytometry every two days. As shown in Fig. 3F, NKG2D. $\zeta$ -NK cells expanded in cocultures (mean  $9.5 \pm 0.7$ -fold increase) with a concomitant reduction in MDSCs (mean  $81.3 \pm 9.4$ -fold decrease), whereas unmodified NK cells failed to expand or eliminate MDSCs. NK cells cultured alone or with autologous monocyte controls did not expand ( $0.8 \pm 0.1$ -fold change). As seen in Fig. 3G, NK cell expansion and MDSC reduction correlated with a shift in the culture cytokine milieu from one that is immune suppressive (more IL6 and IL10; less IFN- $\gamma$  and TNF- $\alpha$ ) in cocultures containing unmodified NK cells, to one that is immune stimulatory and enhances CAR-T antitumor function (less IL6 and IL10; more IFN- $\gamma$  and TNF- $\alpha$ ) in cocultures containing NKG2D. $\zeta$ -NK cells. Hence, NKG2D. $\zeta$ -NK

cells mediate potent cytotoxicity against suppressive MDSCs via their highly expressed NKG2D ligands. In addition, through selective depletion of MDSCs in combination with immune stimulatory cytokine secretion, NKG2D.ζ–NK cells skew the cytokine microenvironment to one that can support CAR-T effector functions (32).

Previous studies have reported that expression of chimeric NKG2D constructs in T lymphocytes can direct these cells to target NKG2D ligand-expressing tumors (16, 33). However, activated T cells (ATCs) themselves upregulate NKG2D ligands (34), with variable ligand expression intensity dependent on the T-cell activation protocol employed, leading to fratricide when the chimeric NKG2D is expressed. To determine if this off-tumor side-effect occurred when the same NKG2D.ζ was expressed in NK cells, we compared the killing of ATCs by autologous NK cells or by autologous T cells expressing our NKG2D.ζ transgene. ATCs and NKG2D.ζ-T cells both upregulated NKG2D ligands during *ex vivo* expansion with CD3/CD28 antibodies plus IL7 and IL15, whereas NKG2D.ζ-transduced NK cells undergoing expansion in our K562-mb15–41BB-L culture system did not (Fig. 3H). Coculture without additional stimulation of NKG2D.ζ-T cells with autologous ATCs produced fratricide, of both the NKG2D.ζ effector T cells ( $35 \pm 7.2\%$  decrease in cell number) and the non-transduced ATC targets ( $98 \pm 11.5\%$  decrease in cell number) ( $n = 3$ ). By contrast, ATC numbers were unaffected by coculture with autologous NKG2D.ζ–NK cells (Fig. 3I). These results show that NK cells expressing NKG2D.ζ can kill autologous MDSCs while sparing other NKG2D ligand expressing populations, thus avoiding the fratricide seen with NKG2D.ζ-expressing T cells.

#### **NKG2D.ζ–NK cells eliminate intra-tumoral MDSCs and reduce tumor burden.**

To determine if NKG2D.ζ–NK cells could eliminate MDSCs from tumor sites *in vivo*, we created an MDSC-containing TME in a xenograft model of neuroblastoma. We chose NKG2D ligand-negative LAN-1 tumor for this experiment so that the effects of NKG2D.ζ–NK cells on MDSCs were not confused with their effects on the tumor cells. LAN-1 tumor cells admixed with human MDSCs were inoculated subcutaneously in NSG mice. These animals had increases in the suppressive cytokines IL10 (10-fold vs. tumor alone) and TGFβ (2.6-fold vs. tumor alone) in circulation by day 16 as compared to animals bearing tumors initiated without MDSCs, and the resultant tumors grew more rapidly due to increased neovascularization and tumor-associated stroma (Supplementary Fig. S3A–D), consistent with clinical reports of MDSC-dense tumors (35). As seen in Fig. 4A, in mice bearing NKG2D ligand-negative tumors without MDSCs, a single infusion of  $1 \times 10^7$  NKG2D.ζ–NK cells resulted in a small delay in tumor growth but eventual progression, suggesting that the LAN-1 tumor itself (a marginally NK-sensitive target) can be killed at higher NK cell doses independent of NKG2D ligand expression. In mice bearing MDSC-containing tumors,  $1 \times 10^7$  NKG2D.ζ–NK cells inhibited tumor growth (Fig. 4B), reduced NKG2D ligand-expressing intra-tumoral MDSCs with only  $8.7 \pm 3.5\%$  of the input MDSCs remaining (Fig. 4C), and prolonged mouse survival (median survival of 73 days vs. 29 days after unmodified NK cells; Fig. 4D). Since LAN-1 tumor cells do not express NKG2D ligands and are only marginally sensitive to ligand-independent lysis, tumors subsequently regrew in these mice once the NKG2D.ζ–NK cells had disappeared (> day 40). Thus, NKG2D.ζ–NK cells can

traffic to tumor sites and reduce intra-tumoral MDSCs but cannot themselves eradicate NKG2D ligand-negative malignant cells in our model.

### **NKG2D.ζ–NK cells secrete chemokines that recruit GD2.CAR-T cells.**

To determine if NKG2D.ζ–NK cells can recruit T cells modified with a tumor-specific CAR to tumor sites containing MDSCs, we cocultured NKG2D.ζ–NK cells with autologous MDSCs and analyzed culture supernatants for chemokines by multiplex ELISA. Compared to unmodified NK cells, NKG2D.ζ–NK cells produce significantly greater CCL5 (RANTES; 10-fold increase), CCL3 (MIP-1α; 2-fold increase), and CCL22 (MDC; 5-fold increase) in response to autologous MDSCs (Fig. 5A). Large amounts of CXCL8 (IL8) were also produced, but there was no significant difference from the production by unmodified NK cells. Analysis of chemokine receptor expression on 2<sup>nd</sup> generation GD2.CAR-T cells revealed CXCR1 (binds CXCL8), CCR2 (binds CCL2), CCR5 (binds CCL3), and CCR4 (binds CCL5) (see Supplementary Fig. S1C). These GD2.CAR-T cells were assayed for chemotaxis to supernatants derived from unmodified or NKG2D.ζ–NK cells cocultured with autologous MDSCs. Supernatants from NKG2D.ζ–NK cell-containing cocultures induced chemotaxis of  $41.1 \pm 5.5\%$  of GD2.CAR-T cells (Fig. 5B), whereas supernatants from unmodified NK cells induced chemotaxis no greater than produced by medium ( $14.9 \pm 6.4\%$  vs.  $17.3 \pm 1.9\%$ , respectively). Chemotaxis was not induced by supernatants from unmodified or NKG2D.ζ–NK cells cocultured with monocytes. Thus, following their encounter with MDSCs, NKG2D.ζ–NK cells secrete chemokines that recruit CAR-Ts *in vitro*.

### **NKG2D.ζ NK cells improve GD2.CAR-T cell trafficking to tumor sites.**

To determine the effects of the MDSC-induced, NKG2D.ζ–NK cell chemokines on CAR-T cell recruitment *in vivo*, we used our MDSC-containing TME xenograft model (see Fig. 4). When tumors reached a volume of  $\sim 100 \text{ mm}^3$  (day 10),  $5 \times 10^6$  NKG2D.ζ–NK cells were infused, followed three days later (day 13) by infusion of  $5 \times 10^6$  luciferase gene-transduced GD2.CAR-T cells. Tumor localization and expansion of GD2.CAR-T cells was measured over time via live-animal bioluminescence imaging. As seen in Fig. 5C, GD2.CAR-T cells injected alone on day 13 after tumor inoculation (without pre-administration of NKG2D.ζ–NK cells) into mice bearing tumors devoid of MDSCs localized effectively to subcutaneous tumors in the flank (4 of 5 mice showed bioluminescent signal on days 14 and 18; Fig. 5C). There was a  $10.5 \pm 0.8$ -fold increase in bioluminescent signal on day 18, with CAR-T cell bioluminescence remaining above baseline levels for the duration of the experiment (Fig. 5D). However, in tumors containing MDSCs, CAR-T cells localized poorly: only 1 of 5 mice exhibited bioluminescent signal (Fig. 5C), with only a  $1.02 \pm 0.1$ -fold increase in bioluminescent signal on day 18 and bioluminescence falling below pre-infusion levels within 10 days after injection (Fig. 5D). In contrast, pre-administration of NKG2D.ζ–NK cells on day 10 into mice bearing MDSC-containing tumors allowed subsequently infused GD2.CAR-T cells to localize effectively to tumor sites, with bioluminescence in 5 of 5 mice at the tumor site and a  $10.9 \pm 0.2$ -fold increase in bioluminescent signal on day 18, within 5 days of injection (Fig. 5D).

To determine if NKG2D.ζ–NK cells could promote GD2.CAR-T infiltration into the tumor bed, we compared the frequency of human GD2.CAR-T and human NK cells in the tumor periphery and the tumor core by immunohistochemistry (Supplementary Fig. S4A–B). In tumors without MDSCs,  $89 \pm 11\%$  of the total T cells in the tumor had infiltrated into the tumor core. In contrast, a much smaller fraction ( $39 \pm 16\%$ ) infiltrated into the core of tumors containing MDSCs, suggesting TME suppression of CAR-T infiltration. However, pre-treatment of tumors containing MDSCs with NKG2D.ζ–NK cells increased the fraction of intra-tumoral CAR-T cells ( $70 \pm 13\%$ ) within the tumor core. Equal numbers of NKG2D.ζ–NK cells were observed within both peripheral and core samples from MDSC-positive and MDSC-negative tumors (Supplementary Fig. S5), suggesting the ability of NK cells to traffic well within tumors despite the presence of MDSCs.

### **Elimination of MDSCs increases antitumor activity of GD2.CAR-T cells.**

To determine if the activities of NKG2D.ζ–NK cells described above enhance the antitumor function of CAR-T cells, we treated mice bearing subcutaneous, luciferase-labeled neuroblastoma containing MDSCs with GD2.CAR-T cells preceded by NKG2D.ζ–NK cells, in a similar set-up to experiments in Fig. 5C. As seen in Fig. 6A–B, a single injection of  $5 \times 10^6$  NKG2D.ζ–NK cells (a dose that achieved intra-tumoral MDSC depletion with only  $26.8 \pm 5.8\%$  of the input MDSCs remaining) resulted in no significant tumor regression or prolongation of survival in mice bearing xenografts containing human MDSCs. A single infusion of  $5 \times 10^6$  GD2.CAR-T cells significantly reduced tumor in mice whose xenografts lacked human MDSCs with a median survival of 95 days (Fig. 6C–D). However, the same GD2.CAR-T cells were ineffective against xenografts containing human MDSCs, worsening overall median survival to 39 days (Fig. 6B). In contrast, when the same GD2.CAR-T cell injection was preceded 3 days earlier by a single injection of  $5 \times 10^6$  NKG2D.ζ–NK cells (that had no direct antitumor effect by themselves within the other arm of the same experiment, see Fig. 6A–B), the antitumor activity of the GD2.CAR-T cells in mice bearing MDSC-containing tumors was restored to the level observed in mice whose tumors lacked MDSCs (Fig. 6C). NKG2D.ζ–NK cells pre-injection also improved the overall survival of the mice with MDSC-containing tumors to a median 120 days with durable cure in 2 of 5 mice (Fig. 6D). Taken together, our results suggest that NKG2D.ζ–NK cells not only eliminate MDSCs from the TME, but also recruit CAR-T cells to intra-tumoral sites which facilitates antitumor efficacy.

## **DISCUSSION**

We have developed a TME-disrupting approach that eliminates MDSCs and rescues MDSC-mediated impairment of tumor-directed CAR-T cells. We show that when co-implanted with a neuroblastoma cell line, human MDSCs both enhance tumor growth and suppress the infiltration, expansion, and antitumor efficacy of tumor-specific CAR T-cells. In this model, NK cells bearing a chimeric version of the activating receptor NKG2D (NKG2D.ζ–NK cells) are directly cytotoxic to autologous MDSCs, thus eliminating MDSCs from tumors. In addition, NKG2D.ζ–NK cells secrete pro-inflammatory cytokines and chemokines in response to MDSCs at the tumor site, improving CAR-T cell infiltration and function, and resulting in tumor regression and prolonged survival compared to treatment with CAR-T

cells alone. Our cell therapy approach utilizes an engineered innate immune effector that targets the TME, and shows potential to enhance efficacy of combination immune-based therapies for solid tumors.

NKG2D.ζ–NK cells directly killed highly suppressive MDSCs generated *in vitro* as well as those from patient tumors. NKG2D.ζ–NK cells also secreted cytokines that favored immune activation in response to MDSCs. Unmodified NK cells were unable to mediate these effects. The ability of NKG2D.ζ–NK cells to eliminate MDSCs from the TME should have several beneficial effects for antitumor immunity. First, as MDSCs express suppressive cytokines such as TGFβ and the checkpoint ligands PDL-1 and PDL-2, elimination of MDSCs should help relieve the suppression of endogenous T cell responses and potentiate the activity of adoptive T cell therapies. Given that high baseline numbers of MDSCs have been reported as a biomarker of poor response in the context of trials with the checkpoint inhibitors ipilimumab and pembrolizumab (36, 37), elimination of MDSCs by NKG2D.ζ–NK cells may also enhance checkpoint inhibition. Second, elimination of MDSCs should also decrease other MDSC-associated effects, including neovascularization via their expression of VEGF, production of immunosuppressive metabolic products such as PGE<sub>2</sub> and adenosine, and establishment of tumor-supportive stroma via their expression of iNOS, FGF, and matrix metalloproteinases (8). In short, the ability of NKG2D.ζ–NK cells to eliminate MDSCs alters the tumor microenvironment in multiple ways that should improve antitumor immunity.

Previous strategies for modulation of MDSCs within the TME have included use of agents that block single functions such as secretion of nitric oxide (38) or expression of checkpoint molecules (39); induce MDSC differentiation such as with all-trans retinoic acid (40); or eliminate MDSCs such as with the cytotoxic agents doxorubicin or cyclophosphamide (41). The MDSC eliminating effects were dependent on continued administration of the agents, with a rapid rebound in MDSCs after discontinuation. Moreover, many of these agents have off-target toxicities that include damage to endogenous tumor-specific T cells. In contrast, NKG2D.ζ–NK cells produce prolonged and specific elimination of MDSCs with the potential to kill MDSCs that are recruited to the tumor from the bone marrow, while continually secreting cytokines and chemokines which respectively alter TME suppression and recruit and activate tumor-specific T cells. Thus, NKG2D.ζ–NK cells exert a prolonged combination of simultaneous immune modulatory effects that enhance antitumor immune function in ways that could not be achieved by previous methods that target MDSCs.

We observed no toxicity against normal hematopoietic cells when NKG2D.ζ was expressed in autologous human NK cells. Previous studies overexpressing an NKG2D.ζ receptor containing co-stimulatory endodomains (e.g., CD28 or 41BB) and DAP10, a signaling adaptor molecule for enhanced surface expression of NKG2D, in T cells showed activity against NKG2D ligand-overexpressing tumors, but at the cost of fratricide *in vitro* and lethal toxicity in mice (16, 33, 34). Using our standard T-cell activation/expansion protocol (22), we also observed upregulation of NKG2D ligands, leading to fratricide in T cells expressing NKG2D.ζ. When NKG2D.ζ–T cells engage NKG2D ligands expressed on normal tissues, they will not receive the physiologic NK cell-directed inhibitory inputs that would safely regulate this potent and unopposed chimeric receptor activity. By contrast, when NKG2D.ζ

is expressed on NK cells, they are able to recognize inhibitory NK cell ligands such as self-MHC expressed on healthy self-tissues, counteracting otherwise unopposed positive signals from NKG2D ligands. Thus, an NK cell platform for NKG2D enhancement may limit toxicity while taking advantage of the cytotoxic and immune modulatory potential of the receptor-ligand system.

Unlike wild-type NKG2D, transgenic NKG2D.ζ expression and activity were not sensitive to down-modulation by TGFβ or soluble NKG2D ligands, allowing improved function in the TME. Native NKG2D relies solely on the intra-cytoplasmic adaptor DAP10 for mediating its cytolytic activity in human NK cells (42). TGFβ1 and soluble NKG2D ligands both decrease DAP10 gene transcription and protein activity, and thus reduce NKG2D function in endogenous NK cells (43, 44). In contrast, transgenic NKG2D.ζ does not rely on DAP10-based signaling for its activity, since signaling occurs through the ζ-chain. Thus, this construct provides a stable cytolytic pathway capable of circumventing TME-mediated down-modulation of native NKG2D activity. A previous study expressing a chimeric NKG2D.ζ molecule that incorporated DAP10 reported enhanced NK cytotoxicity compared to NKG2D.ζ alone *in vitro* against a variety of human cancer cell lines as well as in a xenograft model of osteosarcoma (45). However, this report did not address the susceptibility of this complex to down-modulation by TGFβ or soluble NKG2D ligands, or whether these NK cells had activity against MDSCs.

NKG2D.ζ–NK cells countered immunosuppression mediated by MDSCs leading to enhanced CAR-T cell tumor infiltration and expansion at tumor sites, CAR-T functions that are impaired in patients with solid tumors (46). Unlike the GD2.CAR-T cells in our model, NKG2D.ζ–NK cells homed effectively to MDSC-engrafted tumors and released an array of chemokines that increased T cell infiltration of tumor. Unlike pharmacologic strategies aimed at enhancing leukocyte trafficking, including administration of lymphotactin or TNFα (47), our approach does not require continuous cytokine administration. In fact, the ability of chimeric NKG2D to augment NK immune function specifically within the immunosuppressive TME provides for the local release of chemotactic factors, reflecting a more homeostatic method by which to increase CAR-T infiltration. Once there, CAR-T cells should meet an environment favorably modified by NKG2D.ζ–NK cell mediated elimination of MDSCs and production of pro-inflammatory cytokines. Indeed, elimination of MDSCs from a GD2<sup>+</sup> tumor xenograft enhanced the activity of GD2.CAR-T cells in our model, including T-cell survival and intratumoral expansion. Given the suppressive effects of MDSCs in neuroblastoma (48, 49), the model shows how reversal of an MDSC-mediated suppressive microenvironment can improve antitumor functions of effector T cells.

Clinical neuroblastoma contains intense infiltrates of MDSCs (50), which are not included in tumor xenograft models currently used to study human cell therapeutics. Our data suggest that co-inoculation of tumors with suppressive components (such as MDSCs) can model TME-mediated suppression of CAR-T activity against solid tumors, and provides a method by which to understand and counter immunosuppression. Although NSG mice lack a complete immune system in which to examine the effects of multiple endogenous immune components, our ability to engraft exogenous components (e.g., human MDSCs) within our TME model provides the possibility of simulating different immunosuppressive aspects of

the solid TME. In fact, further model development utilizing human inhibitory macrophages and regulatory T cells (Tregs) as additional suppressive components of the TME is currently underway in our laboratory.

In summary, we describe an approach to reverse the suppressive TME using engineered human NK cells. We have shown that generation and expansion of our NK cell product is feasible and that NKG2D.ζ–NK cells have antitumor activity within a suppressive solid tumor microenvironment without toxicity to normal NKG2D ligand-expressing tissues. Hence, the elimination of suppressive MDSCs by NKG2D.ζ–NK cells may safely enhance adoptive cellular immunotherapy for neuroblastoma and for many other tumors that are supported and protected by MDSCs.

## Supplementary Material

Refer to Web version on PubMed Central for supplementary material.

## ACKNOWLEDGMENTS

The authors would like to thank Dr. Charles L. Sentman (Dartmouth Geisel School of Medicine, Hanover, NH, USA) for providing the retroviral vector encoding the initial NKG2D.ζ. This work was supported, in parts, by the St. Baldrick's Foundation Fellowship Award (R.P.), the Conquer Cancer Foundation Young Investigator Award (R.P.), Hyundai Hope on Wheels Foundation (R.P.), and the American Cancer Society (R.P.). In addition, the authors acknowledge the support of Lisa Rollins at the Center for Cell and Gene Therapy and the Human Tissue Acquisition and Pathology Core of Baylor College of Medicine. We thank Malcolm K. Brenner for expert editorial input.

**Financial Support:** St. Baldrick's Foundation, Conquer Cancer Foundation, Alex's Lemonade Stand Foundation, and American Cancer Society

## Abbreviations used in this paper:

<b>NK</b>	natural killer
<b>MDSC</b>	myeloid-derived suppressor cell
<b>CAR</b>	chimeric antigen receptor
<b>PBMC</b>	peripheral blood mononuclear cell
<b>TME</b>	tumor microenvironment
<b>E:T</b>	effector-to-target ratio
<b>Ab</b>	antibody
<b>APC</b>	antigen-presenting cell
<b>CTL</b>	cytotoxic T lymphocyte
<b>DC</b>	dendritic cell
<b>ATC</b>	activated T cell

## REFERENCES

1. Fesnak AD, June CH, and Levine BL. Engineered T cells: the promise and challenges of cancer immunotherapy. *Nat Rev Cancer*. 2016;16(9):566–81. [PubMed: 27550819]
2. Maude SL, Frey N, Shaw PA, Aplenc R, Barrett DM, Bunin NJ, Chew A, Gonzalez VE, Zheng Z, Lacey SF, et al. Chimeric antigen receptor T cells for sustained remissions in leukemia. *N Engl J Med*. 2014;371(16):1507–17. [PubMed: 25317870]
3. Davila ML, Riviere I, Wang X, Bartido S, Park J, Curran K, Chung SS, Stefanski J, Borquez-Ojeda O, Olszewska M, et al. Efficacy and toxicity management of 19–28z CAR T cell therapy in B cell acute lymphoblastic leukemia. *Sci Transl Med*. 2014;6(224):224ra25.
4. Hege KM, Bergsland EK, Fisher GA, Nemunaitis JJ, Warren RS, McArthur JG, Lin AA, Schlom J, June CH, and Sherwin SA. Safety, tumor trafficking and immunogenicity of chimeric antigen receptor (CAR)-T cells specific for TAG-72 in colorectal cancer. *J Immunother Cancer*. 2017;5(22).
5. Thistlethwaite FC, Gilham DE, Guest RD, Rothwell DG, Pillai M, Burt DJ, Byatte AJ, Kirillova N, Valle JW, Sharma SK, et al. The clinical efficacy of first-generation carcinoembryonic antigen (CEACAM5)-specific CAR T cells is limited by poor persistence and transient pre-conditioning-dependent respiratory toxicity. *Cancer immunology, immunotherapy : CII*. 2017;66(11):1425–36. [PubMed: 28660319]
6. Burga RA, Thorn M, Point GR, Guha P, Nguyen CT, Licata LA, DeMatteo RP, Ayala A, Joseph Espat N, Junghans RP, et al. Liver myeloid-derived suppressor cells expand in response to liver metastases in mice and inhibit the anti-tumor efficacy of anti-CEA CAR-T. *Cancer immunology, immunotherapy : CII*. 2015;64(7):817–29. [PubMed: 25850344]
7. Gabrilovich DI, and Nagaraj S. Myeloid-derived suppressor cells as regulators of the immune system. *Nature reviews Immunology*. 2009;9(3):162–74.
8. Marvel D, and Gabrilovich DI. Myeloid-derived suppressor cells in the tumor microenvironment: expect the unexpected. *J Clin Invest*. 2015;125(9):3356–64. [PubMed: 26168215]
9. Diaz-Montero CM, Salem ML, Nishimura MI, Garrett-Mayer E, Cole DJ, and Montero AJ. Increased circulating myeloid-derived suppressor cells correlate with clinical cancer stage, metastatic tumor burden, and doxorubicin-cyclophosphamide chemotherapy. *Cancer immunology, immunotherapy : CII*. 2009;58(1):49–59. [PubMed: 18446337]
10. Caligiuri MA. Human natural killer cells. *Blood*. 2008;112(3):461–9. [PubMed: 18650461]
11. Ferlazzo G, and Morandi B. Cross-Talks between Natural Killer Cells and Distinct Subsets of Dendritic Cells. *Front Immunol*. 2014;5(159).
12. Stojanovic A, and Cerwenka A. Natural killer cells and solid tumors. *Journal of innate immunity*. 2011;3(4):355–64. [PubMed: 21502747]
13. Gonzalez S, Lopez-Soto A, Suarez-Alvarez B, Lopez-Vazquez A, and Lopez-Larrea C. NKG2D ligands: key targets of the immune response. *Trends Immunol*. 2008;29(8):397–403. [PubMed: 18602338]
14. Raffaghello L, Prigione I, Airoidi I, Camoriano M, Levreri I, Gambini C, Pende D, Steinle A, Ferrone S, and Pistoia V. Downregulation and/or release of NKG2D ligands as immune evasion strategy of human neuroblastoma. *Neoplasia*. 2004;6(5):558–68. [PubMed: 15548365]
15. Dasgupta S, Bhattacharya-Chatterjee M, O'Malley BW Jr., and Chatterjee SK. Inhibition of NK cell activity through TGF-beta 1 by down-regulation of NKG2D in a murine model of head and neck cancer. *J Immunol*. 2005;175(8):5541–50. [PubMed: 16210663]
16. Barber A, Rynda A, and Sentman CL. Chimeric NKG2D expressing T cells eliminate immunosuppression and activate immunity within the ovarian tumor microenvironment. *J Immunol*. 2009;183(11):6939–47. [PubMed: 19915047]
17. Heczey A, Liu D, Tian G, Courtney AN, Wei J, Marinova E, Gao X, Guo L, Yvon E, Hicks J, et al. Invariant NKT cells with chimeric antigen receptor provide a novel platform for safe and effective cancer immunotherapy. *Blood*. 2014;124(18):2824–33. [PubMed: 25049283]
18. Zhang T, Barber A, and Sentman CL. Generation of antitumor responses by genetic modification of primary human T cells with a chimeric NKG2D receptor. *Cancer Res*. 2006;66(11):5927–33. [PubMed: 16740733]

19. Shaffer DR, Savoldo B, Yi Z, Chow KK, Kakarla S, Spencer DM, Dotti G, Wu MF, Liu H, Kenney S, et al. T cells redirected against CD70 for the immunotherapy of CD70-positive malignancies. *Blood*. 2011;117(16):4304–14. [PubMed: 21304103]
20. Kelly PF, Carrington J, Nathwani A, and Vanin EF. RD114-pseudotyped oncoretroviral vectors. Biological and physical properties. *Ann N Y Acad Sci*. 2001;938(262–76; discussion 76–7).
21. Lapteva N, Durett AG, Sun J, Rollins LA, Huye LL, Fang J, Dandekar V, Mei Z, Jackson K, Vera J, et al. Large-scale ex vivo expansion and characterization of natural killer cells for clinical applications. *Cytotherapy*. 2012;14(9):1131–43. [PubMed: 22900959]
22. Xu Y, Zhang M, Ramos CA, Durett A, Liu E, Dakhova O, Liu H, Creighton CJ, Gee AP, Heslop HE, et al. Closely related T-memory stem cells correlate with in vivo expansion of CAR-CD19-T cells and are preserved by IL-7 and IL-15. *Blood*. 2014;123(24):3750–9. [PubMed: 24782509]
23. Lechner MG, Liebertz DJ, and Epstein AL. Characterization of cytokine-induced myeloid-derived suppressor cells from normal human peripheral blood mononuclear cells. *J Immunol*. 2010;185(4):2273–84. [PubMed: 20644162]
24. Bronte V, Brandau S, Chen SH, Colombo MP, Frey AB, Greten TF, Mandruzzato S, Murray PJ, Ochoa A, Ostrand-Rosenberg S, et al. Recommendations for myeloid-derived suppressor cell nomenclature and characterization standards. *Nat Commun*. 2016;7(12150).
25. Kruisbeek AM, Shevach E, and Thornton AM. Proliferative assays for T cell function. *Curr Protoc Immunol*. 2004;Chapter 3(Unit 3 12).
26. Roda JM, Parihar R, Magro C, Nuovo GJ, Tridandapani S, and Carson WE. Natural killer cells produce T cell-recruiting chemokines in response to antibody-coated tumor cells. *Cancer Res*. 2006;66(1):517–26. [PubMed: 16397268]
27. Charo J, Perez C, Buschow C, Jukica A, Czeh M, and Blankenstein T. Visualizing the dynamic of adoptively transferred T cells during the rejection of large established tumors. *Eur J Immunol*. 2011;41(11):3187–97. [PubMed: 21898380]
28. Miller JS, Rooney CM, Curtsinger J, McElmurry R, McCullar V, Verneris MR, Lapteva N, McKenna D, Wagner JE, Blazar BR, et al. Expansion and Homing of Adoptively Transferred Human Natural Killer Cells in Immunodeficient Mice Varies with Product Preparation and In Vivo Cytokine Administration: Implications for Clinical Therapy. *Biology of blood and marrow transplantation : journal of the American Society for Blood and Marrow Transplantation*. 2014.
29. Miller JS, Rooney CM, Curtsinger J, McElmurry R, McCullar V, Verneris MR, Lapteva N, McKenna D, Wagner JE, Blazar BR, et al. Expansion and homing of adoptively transferred human natural killer cells in immunodeficient mice varies with product preparation and in vivo cytokine administration: implications for clinical therapy. *Biology of blood and marrow transplantation : journal of the American Society for Blood and Marrow Transplantation*. 2014;20(8):1252–7.
30. Groh V, Wu J, Yee C, and Spies T. Tumour-derived soluble MIC ligands impair expression of NKG2D and T-cell activation. *Nature*. 2002;419(6908):734–8. [PubMed: 12384702]
31. Markowitz J, Wesolowski R, Papenfuss T, Brooks TR, and Carson WE. Myeloid-derived suppressor cells in breast cancer. *Breast Cancer Res Treat*. 2013;140(1):13–21. [PubMed: 23828498]
32. Xue Q, Bettini E, Paczkowski P, Ng C, Kaiser A, McConnell T, Kodrasi O, Quigley MF, Heath J, Fan R, et al. Single-cell multiplexed cytokine profiling of CD19 CAR-T cells reveals a diverse landscape of polyfunctional antigen-specific response. *J Immunother Cancer*. 2017;5(1):85. [PubMed: 29157295]
33. Spear P, Barber A, Rynda-Apple A, and Sentman CL. Chimeric antigen receptor T cells shape myeloid cell function within the tumor microenvironment through IFN- $\gamma$  and GM-CSF. *J Immunol*. 2012;188(12):6389–98. [PubMed: 22586039]
34. VanSeggelen H, Hammill JA, Dvorkin-Gheva A, Tantalò DG, Kwiecien JM, Denisova GF, Rabinovich B, Wan Y, and Bramson JL. T Cells Engineered With Chimeric Antigen Receptors Targeting NKG2D Ligands Display Lethal Toxicity in Mice. *Molecular therapy : the journal of the American Society of Gene Therapy*. 2015;23(10):1600–10. [PubMed: 26122933]
35. Qu P, Wang LZ, and Lin PC. Expansion and functions of myeloid-derived suppressor cells in the tumor microenvironment. *Cancer Lett*. 2016;380(1):253–6. [PubMed: 26519756]

36. Martens A, Wistuba-Hamprecht K, Geukes Foppen M, Yuan J, Postow MA, Wong P, Romano E, Khammari A, Dreno B, Capone M, et al. Baseline Peripheral Blood Biomarkers Associated with Clinical Outcome of Advanced Melanoma Patients Treated with Ipilimumab. *Clin Cancer Res.* 2016;22(12):2908–18. [PubMed: 26787752]
37. Weide B, Martens A, Hassel JC, Berking C, Postow MA, Bisschop K, Simeone E, Mangana J, Schilling B, Di Giacomo AM, et al. Baseline Biomarkers for Outcome of Melanoma Patients Treated with Pembrolizumab. *Clin Cancer Res.* 2016;22(22):5487–96. [PubMed: 27185375]
38. Jayaraman P, Parikh F, Lopez-Rivera E, Hailemichael Y, Clark A, Ma G, Cannan D, Ramacher M, Kato M, Overwijk WW, et al. Tumor-expressed inducible nitric oxide synthase controls induction of functional myeloid-derived suppressor cells through modulation of vascular endothelial growth factor release. *J Immunol.* 2012;188(11):5365–76. [PubMed: 22529296]
39. Serafini P, Meckel K, Kelso M, Noonan K, Califano J, Koch W, Dolcetti L, Bronte V, and Borrello I. Phosphodiesterase-5 inhibition augments endogenous antitumor immunity by reducing myeloid-derived suppressor cell function. *J Exp Med.* 2006;203(12):2691–702. [PubMed: 17101732]
40. Mirza N, Fishman M, Fricke I, Dunn M, Neuger AM, Frost TJ, Lush RM, Antonia S, and Gabrilovich DI. All-trans-retinoic acid improves differentiation of myeloid cells and immune response in cancer patients. *Cancer Res.* 2006;66(18):9299–307. [PubMed: 16982775]
41. Alizadeh D, Katsanis E, and Larmonier N. Chemotherapeutic targeting of myeloid-derived suppressor cells. *Oncoimmunology.* 2014;3(1):e27359. [PubMed: 24653963]
42. Roda-Navarro P, and Reyburn HT. The traffic of the NKG2D/Dap10 receptor complex during natural killer (NK) cell activation. *J Biol Chem.* 2009;284(24):16463–72. [PubMed: 19329438]
43. Park YP, Choi SC, Kiesler P, Gil-Krzewska A, Borrego F, Weck J, Krzewski K, and Coligan JE. Complex regulation of human NKG2D-DAP10 cell surface expression: opposing roles of the gammac cytokines and TGF-beta1. *Blood.* 2011;118(11):3019–27. [PubMed: 21816829]
44. Coudert JD, Zimmer J, Tomasello E, Cebecauer M, Colonna M, Vivier E, and Held W. Altered NKG2D function in NK cells induced by chronic exposure to NKG2D ligand-expressing tumor cells. *Blood.* 2005;106(5):1711–7. [PubMed: 15886320]
45. Chang YH, Connolly J, Shimasaki N, Mimura K, Kono K, and Campana D. A chimeric receptor with NKG2D specificity enhances natural killer cell activation and killing of tumor cells. *Cancer Res.* 2013;73(6):1777–86. [PubMed: 23302231]
46. Moon EK, Wang LC, Dolfi DV, Wilson CB, Ranganathan R, Sun J, Kapoor V, Scholler J, Pure E, Milone MC, et al. Multifactorial T-cell hypofunction that is reversible can limit the efficacy of chimeric antigen receptor-transduced human T cells in solid tumors. *Clin Cancer Res.* 2014;20(16):4262–73. [PubMed: 24919573]
47. Cairns CM, Gordon JR, Li F, Baca-Estrada ME, Moyana T, and Xiang J. Lymphotoxin expression by engineered myeloma cells drives tumor regression: mediation by CD4+ and CD8+ T cells and neutrophils expressing XCR1 receptor. *J Immunol.* 2001;167(1):57–65. [PubMed: 11418632]
48. Gowda M, Payne KK, Godder K, and Manjili MH. HLA-DR expression on myeloid cells is a potential prognostic factor in patients with high-risk neuroblastoma. *Oncoimmunology.* 2013;2(10):e26616. [PubMed: 24349875]
49. Pistoia V, Morandi F, Bianchi G, Pezzolo A, Prigione I, and Raffaghello L. Immunosuppressive microenvironment in neuroblastoma. *Frontiers in oncology.* 2013;3(167).
50. Heczey A, Louis CU, Savoldo B, Dakhova O, Durett A, Grilley B, Liu H, Wu MF, Mei Z, Gee A, et al. CAR T Cells Administered in Combination with Lymphodepletion and PD-1 Inhibition to Patients with Neuroblastoma. *Molecular therapy : the journal of the American Society of Gene Therapy.* 2017.

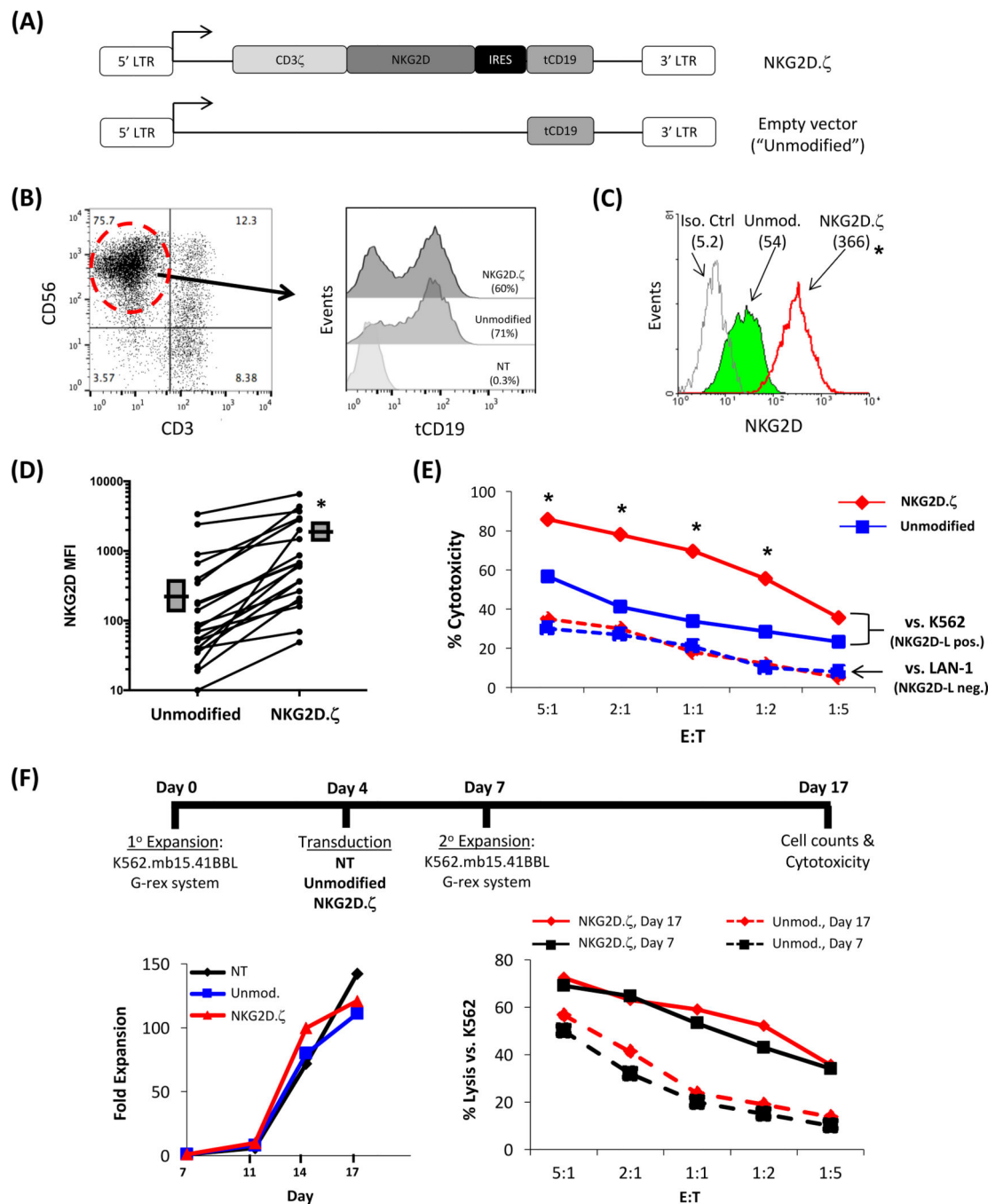


**Figure 1. NKG2D.ζ–NK cells expand and kill ligand-expressing targets.**

(A) Schematic of SFG-based retroviral vector constructs for transduction of human NK cells. (B) Human NK cells were expanded as described in Methods and percentage of CD56<sup>+</sup>/CD3<sup>-</sup> NK cells at time of retroviral transduction (day 4) is shown. Expanded NK cells (red circle in A) purified via depletion of CD3<sup>+</sup> cells were transduced with NKG2D.ζ retroviral vector or empty vector control (referred to as “unmodified”), and transduction efficiencies are shown inset. (C) NKG2D expression on NK cells (MFI, inset) was assessed with isotype antibody as control. Non-transduced NK cells exhibited similar NKG2D

expression to empty vector-transduced NK cells. \*  $p = 0.003$  vs. unmodified condition. **(D)** Expression of NKG2D (absolute MFI on y-axis) on NK cells from each donor ( $n = 25$ ) transduced with either empty vector or NKG2D. $\zeta$  construct was determined by flow cytometry. Each pair of data points connected by a line represent cells from a single donor, to confirm surface expression of our chimeric molecule after transduction. Black line with grey block next to each group are mean MFI  $\pm$  SEM. **(E)** NKG2D. $\zeta$ -NK cell cytotoxicity against K562 and LAN-1 tumor targets in a 4-hour  $^{51}\text{Cr}$ -release assay. Given that K562 and LAN-1 are both NK-sensitive targets, low E:T ratios were utilized to observe differences. Experiment is representative of at least three separate determinations from  $n = 10$  donors. \*  $p < 0.01$  vs. unmodified NK cells at same E:T ratio. **(F)** NKG2D. $\zeta$ -NK cells were expanded after transduction culture (as shown in schema), and fold-expansion and cytotoxicity both pre- (day 7) and post- (day 17) secondary expansion were determined.

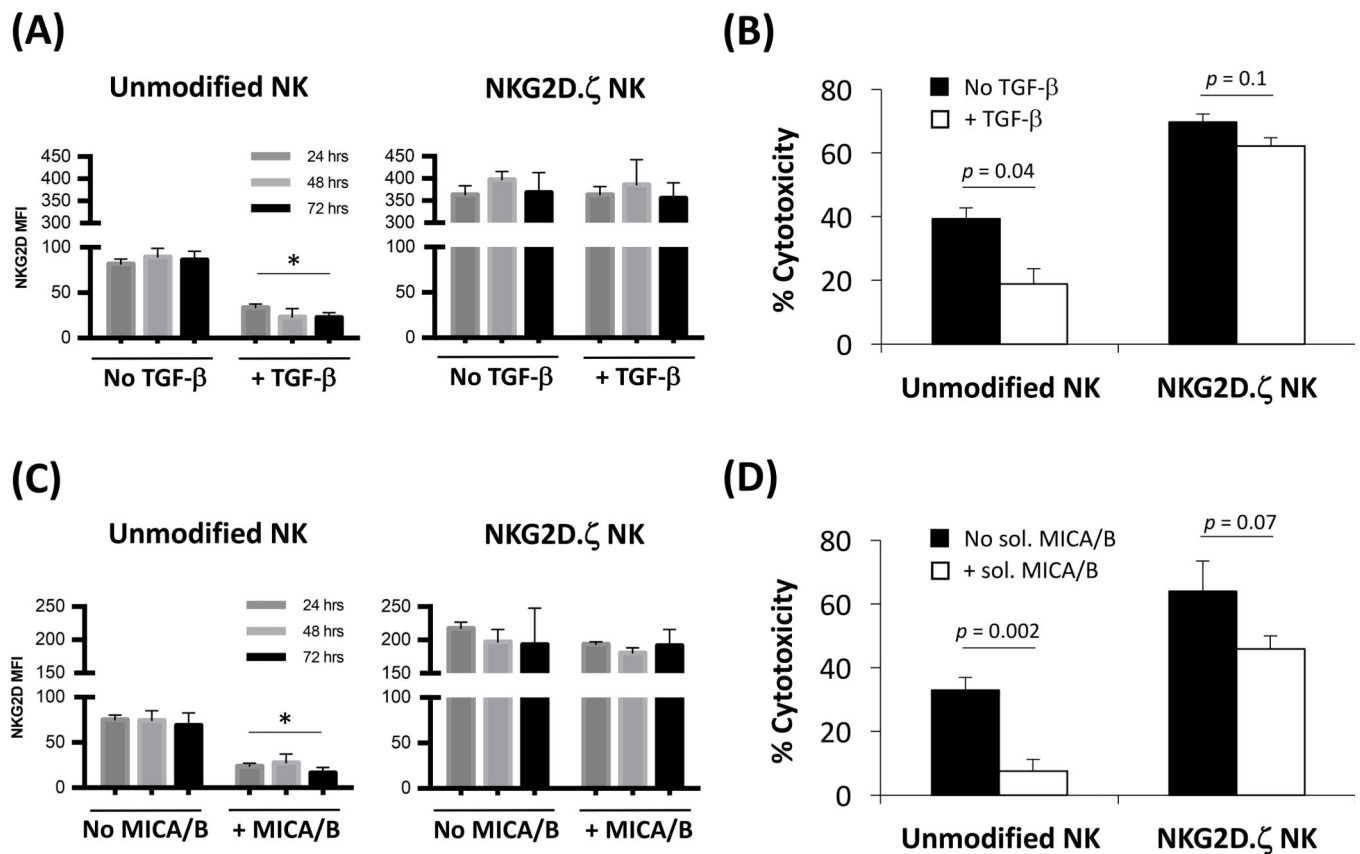


**Figure 2. Transgenic NKG2D.ζ is unaffected by TGFβ or soluble NKG2D ligands.**

NKG2D.ζ or unmodified NK cells ( $n = 5$  donors) were cultured in the presence of TGFβ (5 ng/mL) (A, B) or the soluble NKG2D ligands MICA and MICB (C, D) for 24-, 48-, and 72-hours. NKG2D receptor expression was determined by flow cytometry and NK cytotoxicity against K562 targets was assessed in a 4-hr Cr-release assay at an 5:1 E:T ratio using 48-hr exposed NK cells. Viability of transduced NK cells after exposure to TGFβ for 24, 48, and 72 hours, as assessed by 7-AAD vital staining, was > 90%. \*  $p = 0.001$  vs. non-TGFβ/MICA-treated NK groups at same time-points.

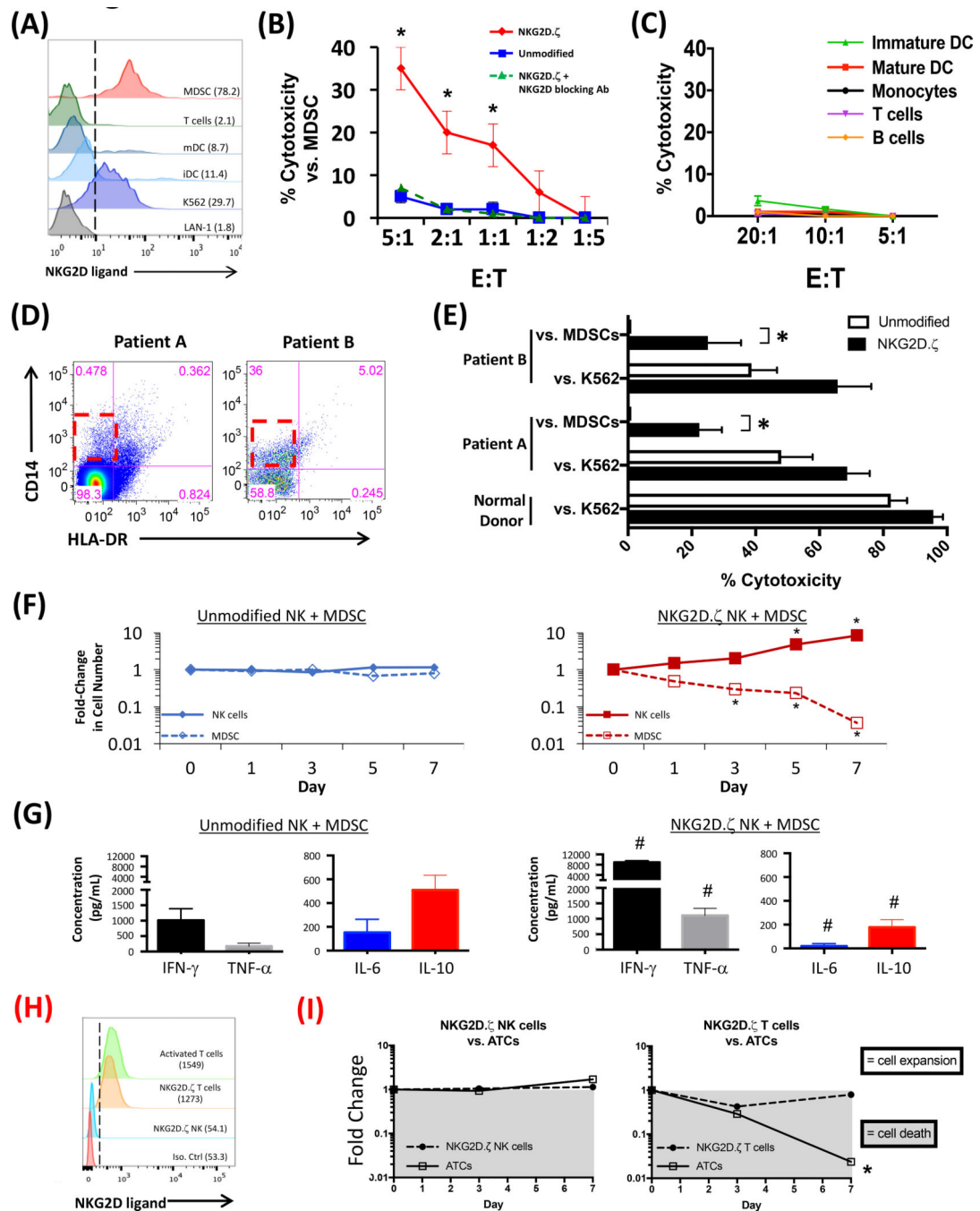


**Figure 3. Human MDSCs express ligands for NKG2D and are killed by NKG2D.ζ-NK cells.** (A) NKG2D ligand expression on human MDSCs by flow cytometry. Immature dendritic cells (iDC) and mature DCs (mDC) were used as myeloid controls. T cells activated with CD3 and CD28 mAbs plus 100 IU/mL IL2 for 24 hours were used as lymphocyte control. LAN-1 and K562 cells were used as negative and positive controls, respectively. MFI of NKG2D ligand expression in parenthesis. Representative data from single donor (of n = 25 normal donors). Isotype control for NKG2D staining routinely fell within the 1<sup>st</sup> log. (B) NKG2D.ζ-NK cell cytotoxicity against autologous MDSCs as targets in a 4-hour <sup>51</sup>Cr-

release assay. In some wells of the cytotoxicity assay, a blocking mAb to NKG2D was added. Representative data from triplicate samples per data point from a single donor (of  $n = 25$  normal donors) is shown. \*  $p < 0.01$  vs. unmodified NK cells at same E:T ratio. (C) In the same experiment as (B), the same batch of NKG2D.ζ–NK cells were analyzed for cytotoxicity against autologous B cells, monocytes, monocyte-derived iDC and mDC, and activated T cells ( $n = 10$  donors examined). (D) M-MDSC frequency by flow cytometry from neuroblastoma tumor samples obtained from high-risk patients, as described in Methods. (E) Cytotoxicity by NKG2D.ζ–NK cells derived from patient PBMC (harvested and frozen at time of tumor sampling) against autologous tumor-derived MDSCs in a 4-hour  $^{51}\text{Cr}$ -release assay. Data shown are from triplicate samples per data point at a 10:1 E:T ratio. \*  $p < 0.001$  vs. unmodified NK cells from same donor. (F) NKG2D.ζ–NK cells were cocultured with autologous MDSCs at 1:1 ratio plus low-dose 50 IU/mL IL2 to maintain NK survival, and fold change in the number of each cell type from the start of coculture was determined by flow cytometry at indicated time-points. \*  $p < 0.001$  vs. NK/MDSC fold-change in unmodified NK cell cocultures. (G) Cell-free supernatants were harvested from cocultures at day 3 and analyzed for IFN $\gamma$ , TNF $\alpha$ , IL6, and IL10 by ELISA. #  $p < 0.01$  vs. corresponding cytokine in cocultures with unmodified NK cells. (H) NKG2D ligand expression was determined for activated T cells (ATCs) expressing NKG2D.ζ and NKG2D.ζ–NK cells. Expression of NKG2D ligands on non-transduced ATCs as control for T-cell activation. (I) NKG2D.ζ–NK cells or NKG2D.ζ T cells were cocultured with autologous ATCs at 1:1 ratio and fold change in the number of each cell type from the start of coculture was determined by flow cytometry at indicated time-points. \*  $p < 0.001$  vs. ATC fold-change at days 0 and 3 cocultures.

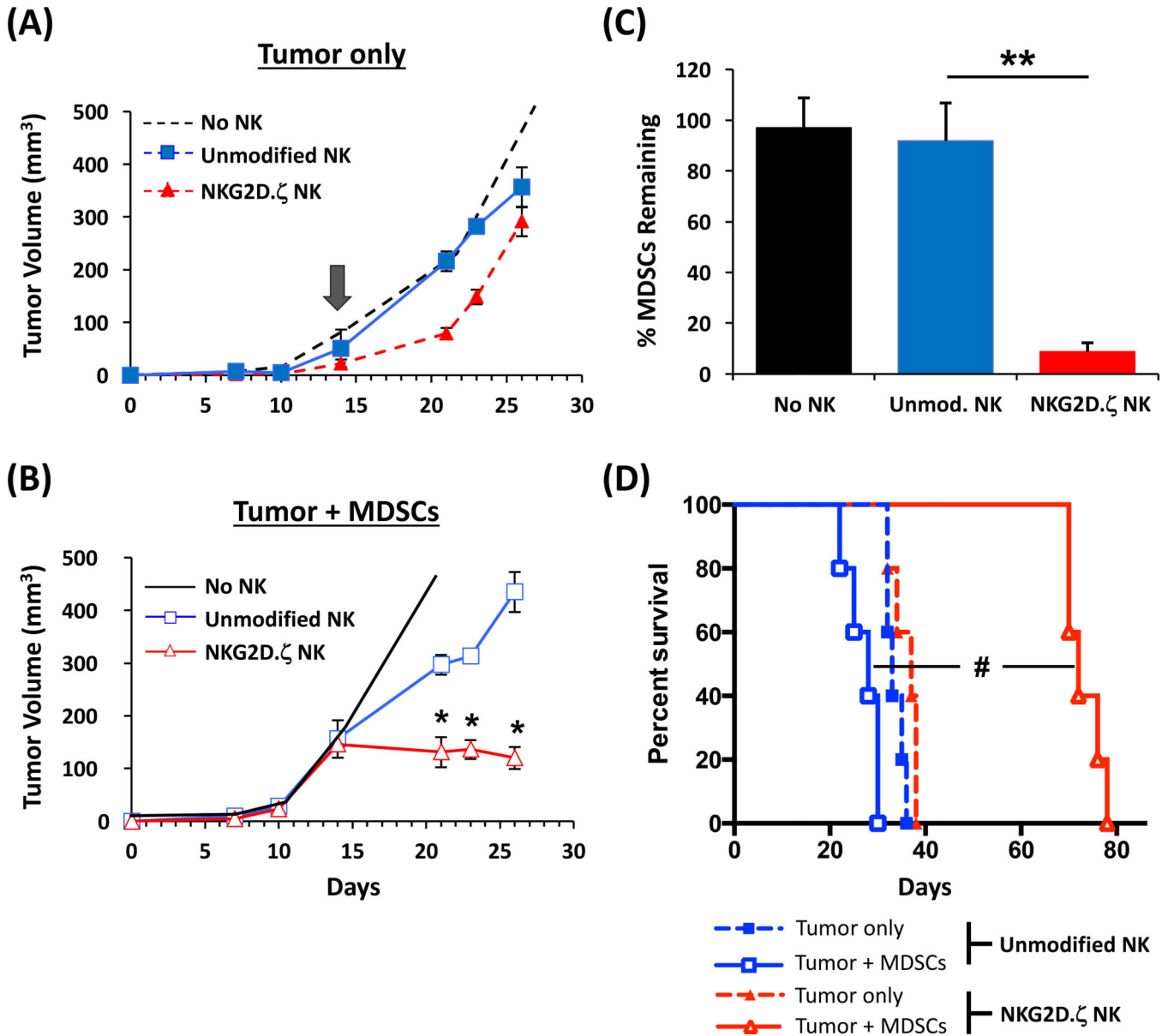


**Figure 4. NKG2D.ζ-NK cells eliminate intra-tumoral MDSCs and reduce tumor burden.** LAN-1 tumor cells, either alone (A) or admixed with human MDSCs (B), were injected S.C. in the flanks of NSG mice. When tumors reached a volume of approx. 100 mm<sup>3</sup> (day 14, gray block arrow inset), no NK cells (PBS control), 1×10<sup>7</sup> unmodified or NKG2D.ζ-NK cells were injected I.V. and tumor growth was measured over time via calipers. \* *p* < 0.03 vs. other conditions shown at same time point. (C) On day 26, intra-tumoral human MDSCs (CD33<sup>+</sup>, HLA-DR<sup>low</sup>) were enumerated by flow cytometry and are presented as mean % MDSCs remaining per treatment group. \*\* *p* < 0.005 vs. unmodified NK treatment. (D) Survival of groups by Kaplan-Meier analysis. # *p* = 0.024. Representative experiment of three performed.

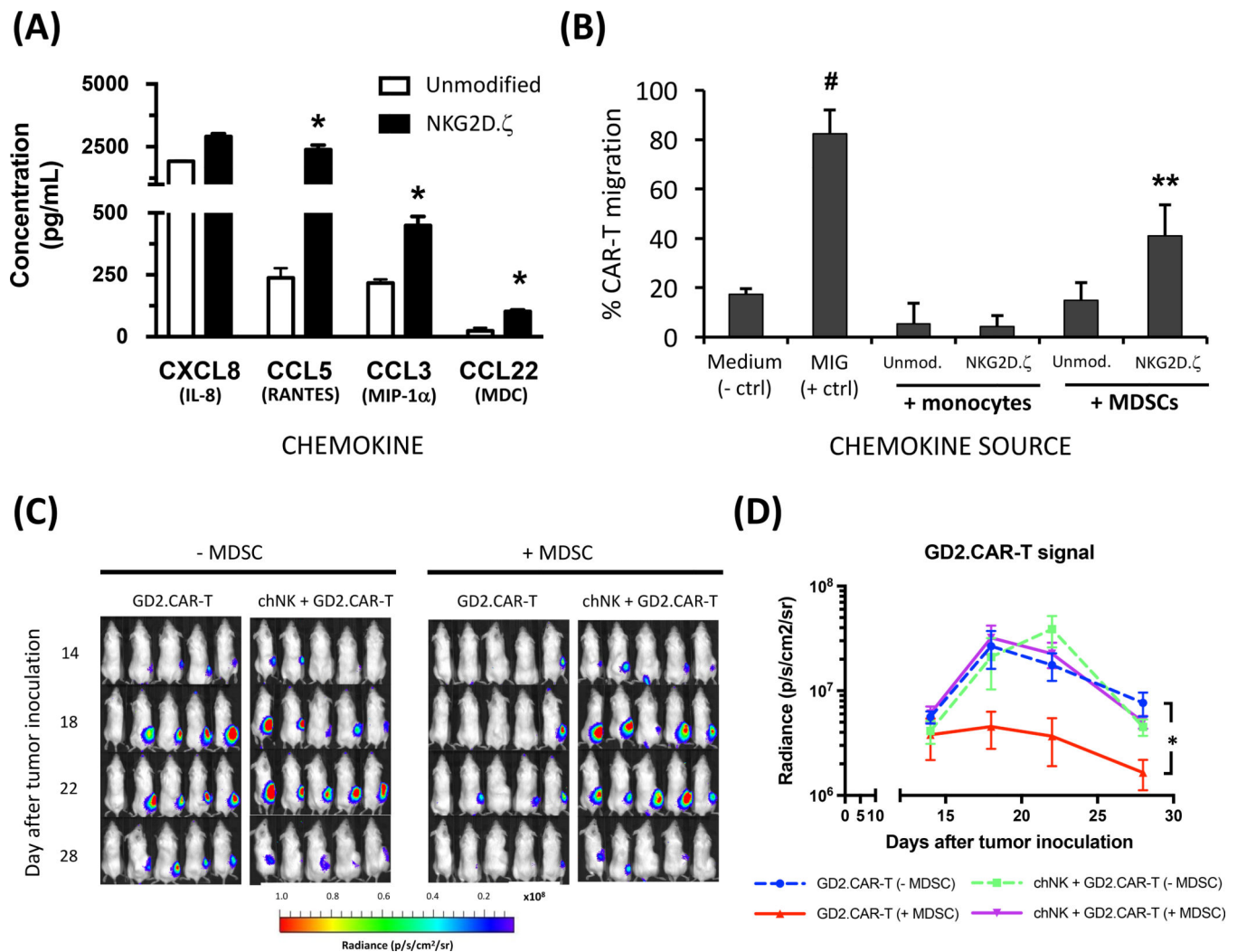


**Figure 5. NKG2D.ζ-NK cells secrete chemokines that recruit GD2.CAR-T cells.**

(A) NKG2D.ζ or unmodified NK cells were cocultured with autologous MDSCs and cell-free culture supernatants harvested at 48 hours were analyzed for chemokines CXCL8, CCL5, CCL3, and CCL22 by ELISA. Shown are mean chemokine concentration  $\pm$  SEM for  $n = 5$  cocultures/donor (data from one of five representative donors is shown). \*  $p < 0.005$  vs. unmodified NK cocultures. (B) GD2.CAR-T cells were assayed for chemotaxis in Transwells (described in Methods) in response to supernatants derived from unmodified or NKG2D.ζ-NK cells cocultured with autologous MDSCs. Supernatants derived from monocyte (non-suppressive myeloid cell control)-stimulated NK cells were also used. #  $p < 0.001$  vs. Medium, \*\*  $p = 0.009$  vs. “unmodified NK plus MDSCs” condition. (C) LAN-1 tumor cells, alone or admixed with human MDSCs, were injected S.C. into the flank of NSG mice. When tumors reached a volume  $\sim 100$  mm<sup>3</sup>,  $5 \times 10^6$  GD2.CAR-T cells were injected I.V. alone on day 13 (GD2.CAR-T), or preceded by  $5 \times 10^6$  NKG2D.ζ-NK cells I.V. injected on day 10 (chNK + GD2.CAR-T). GD2.CAR-T signal at tumor site was measured over time via live-animal bioluminescence imaging. (D) Shown is mean  $\pm$  SEM ( $n = 5$  mice/group)

bioluminescent signal of GD2.CAR-T cells expressed as radiance. \*  $p = 0.01$  vs. all other groups.

Author Manuscript

Author Manuscript

Author Manuscript

Author Manuscript

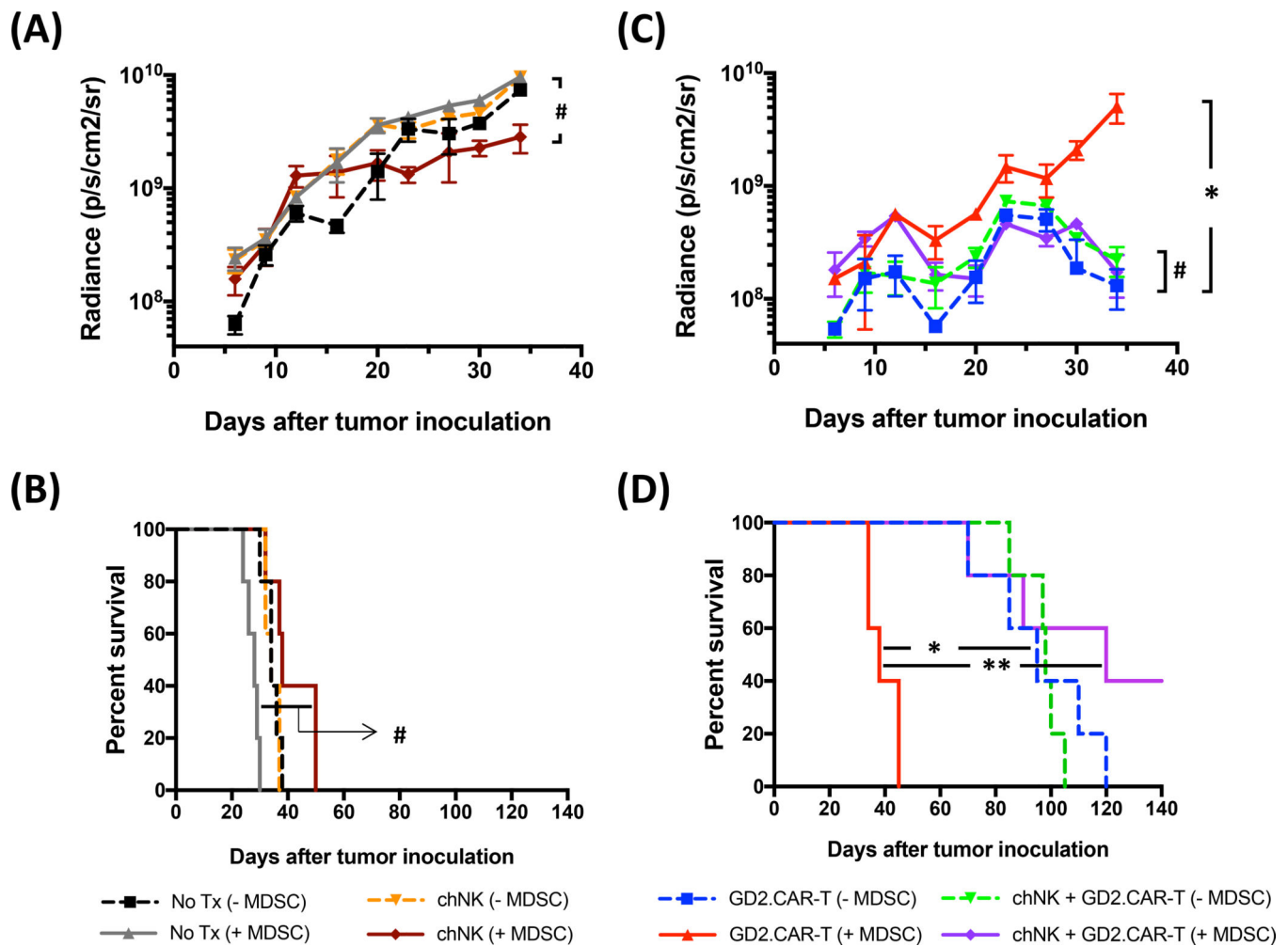


**Figure 6. Elimination of MDSCs by NKG2D.ζ-NK cells increases antitumor activity of GD2.CAR-T cells.**

Luciferase gene-transduced LAN-1 tumor cells, alone or admixed with human MDSCs, were injected S.C. into NSG mice. **(A)** When tumors reached a volume  $\sim 100 \text{ mm}^3$ , no treatment (No Tx; PBS control) or  $5 \times 10^6$  NKG2D.ζ-NK cells alone (chNK) were injected I.V. on day 10 and tumor growth was measured over time via live-animal bioluminescence imaging. Shown is mean  $\pm$  SEM ( $n=5$  mice/group) bioluminescent signal expressed as radiance. # ns,  $p = 0.18$  vs. No treatment (+MDSC) group. **(B)** Survival of groups in A was determined by Kaplan-Meier analysis. # ns,  $p = 0.059$ . **(C)** In other groups of mice within the same experiment,  $5 \times 10^6$  GD2.CAR-T cells were injected I.V. alone on day 13 (GD2.CAR-T), or preceded by  $5 \times 10^6$  NKG2D.ζ-NK cells injected on day 10 (chNK + GD2.CAR-T). \*  $p = 0.001$ ; # ns,  $p = 0.59$  vs. each other. **(D)** Survival of groups in C by Kaplan-Meier analysis. Representative experiment of 5 separate experiments. \*  $p = 0.002$ ; \*\*  $p = 0.001$ .